

Parametric Driving of Dark Solitons in Atomic Bose-Einstein Condensates

N.P. Proukakis[†], N.G. Parker[†], C.F. Barenghi[‡], and C.S. Adams[†]

[†] Department of Physics, University of Durham,
South Road, Durham, DH1 3LE, United Kingdom and
[‡] School of Mathematics and Statistics, University of Newcastle,
Newcastle upon Tyne, NE1 7RU, United Kingdom

A dark soliton oscillating in an elongated harmonically-confined atomic Bose-Einstein condensate continuously interacts, and exchanges energy, with the sound field. By employing periodic optical ‘paddles’ to controllably enhance the sound density, significant energy can be transferred to the soliton, analogous to parametric driving employed in other systems. In the absence of damping, a fast soliton can be essentially stopped, while in the presence of dissipation, driving can lead to a significant extension of soliton lifetimes.

PACS numbers: 03.75.Lm, 05.45.Yv, 42.81.Dp and 47.35.+i

Dark solitons [1] are an important manifestation of the intrinsic nonlinearity of a system and arise in diverse systems such as optical fibers [2], waveguides [3], surfaces of shallow liquids [4], magnetic films [5], and harmonically confined atomic Bose-Einstein Condensates (BECs) [6]. Dark solitons are known to be dynamically unstable in higher than one-dimensional (1D) manifolds (e.g. snake instability in 3D systems leading to a decay into vortex rings [7, 8]). Solitons in 1D geometries experience other instabilities, whose nature depends on the details of the system: For example, dark solitons in optical media are prone to nonlinearity-induced changes in the refractive index [1], whereas in harmonically trapped atomic BECs they experience dynamical instabilities due to the longitudinal confinement [9, 10, 11, 12, 13, 14, 15], as well as thermodynamic [16] and quantum [17] effects. Instabilities lead to dissipation, which manifests itself in the emission of radiation [18] and the subsequent soliton decay. Compensation against dissipative losses by parametric driving has already been demonstrated in some of the above media [4, 19, 20, 21, 22, 23]. The aim of this Letter is to discuss this effect in the context of atomic BECs.

In atomic gases, the snake instability [8] can be suppressed in elongated, quasi-one-dimensional (quasi-1D) geometries [24], whereas thermal instabilities are minimized by considering very low temperatures $T \ll T_c$ (where T_c the BEC transition temperature). In this limit, a dark soliton oscillating in a harmonically confined BEC continuously emits radiation (in the form of sound waves) due to the inhomogeneous background density [9]. The sound remains confined and re-interacts with the soliton, leading to periodic oscillations of the soliton energy [13]. In this Letter we propose the controlled amplification of the background sound field, and illustrate the resulting transfer of energy into the soliton, in close analogy to established parametric driving techniques [4]. Energy is pumped into the sound field via periodically-modulated ‘paddles’, located towards the condensate edge (Fig. 1). If the drive frequency is nearly resonant with the soliton oscillation frequency, the resulting beating effect between the soliton and the sound can lead to the transfer of significant energy into the soliton (for suitably opti-

mized drive parameters). In the absence of dissipation, we demonstrate that an initially fast soliton can be essentially stopped, while under dissipative conditions, the soliton lifetime is shown to be greatly enhanced.

Our analysis is based on the cylindrically-symmetric 3D Gross-Pitaevskii Equation (GPE) describing the evolution of the macroscopic order parameter ψ of an elongated three-dimensional atomic BEC [25]

$$i\hbar \frac{\partial \psi}{\partial t} = -\frac{\hbar^2}{2m} \nabla^2 \psi + V\psi + g|\psi|^2\psi - \mu\psi. \quad (1)$$

where m is the atomic mass, $V = V_T(\mathbf{r}) + V_D(\mathbf{r})$, $V_T(\mathbf{r}) = (m/2)(\omega_z^2 z^2 + \omega_\perp^2 \rho^2)$ is the harmonic confining potential of longitudinal (transverse) frequency ω_z (ω_\perp), where $\omega_z \ll \omega_\perp$, and $V_D(\mathbf{r})$ is the drive potential (Eq. (3)). The nonlinearity arises from atomic interactions yielding a scattering amplitude $g = 4\pi\hbar^2 a/m$, where a is the s -wave scattering length. In this work, $a > 0$, i.e. effective repulsive atomic interactions. The chemical potential is given by $\mu = gn_0$, where n_0 is the peak atomic density.

Dark soliton solutions are supported by the 1D form of Eq. (1) in the absence of external confinement ($V = 0$) [26]. In particular, on a uniform background density n ,

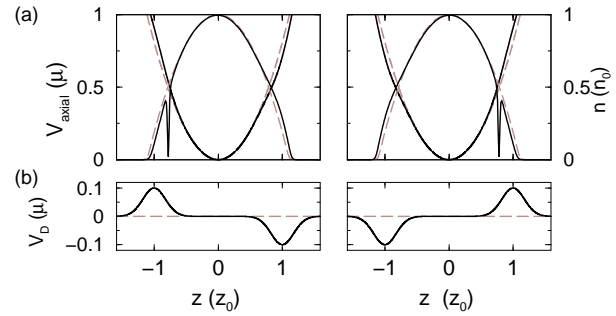


FIG. 1: Schematic of parametric driving: (a) Total axial potential (left axis) and density (right axis) of perturbed harmonic trap with propagating dark soliton (black lines), at two times (left/right plots) corresponding to maximum drive amplitudes. (b) Corresponding drive potentials (black, $\alpha > 0$). The dashed grey lines correspond to an unperturbed trap without a soliton.

a dark soliton with speed v and position $(z - vt)$ has the analytical form,

$$\psi(z, t) = \sqrt{n} e^{-i(\mu/\hbar)t} \left(\beta \tanh \left[\beta \frac{(z - vt)}{\xi} \right] + i \left(\frac{v}{c} \right) \right) \quad (2)$$

where $\beta = \sqrt{1 - (v/c)^2}$, and the healing length $\xi = \hbar/\sqrt{\mu m}$ characterises the soliton width. The soliton speed $v/c = \sqrt{1 - (n_d/n)} = \cos(S/2)$ depends on the total phase slip S across the centre and the soliton depth n_d (with respect to the background density), with the limiting value being set by the Bogoliubov speed of sound $c = \sqrt{\mu/m}$. The energy of the unperturbed dark soliton of Eq. (2) is given by $E_s^0 = (4/3)\hbar cn(1 - (v/c)^2)^{3/2}$. The drive potential

$$V_D = \alpha \sin(\omega_D t) \left[e^{-(z+z_0)^2/w_0^2} - e^{-(z-z_0)^2/w_0^2} \right] \quad (3)$$

consists of two periodically modulated gaussian ‘paddles’, with maximum amplitude α , at opposing positions $\pm z_0$ from the trap centre, and oscillating in anti-phase at a frequency ω_D (Fig. 1). Such a set-up could be created by time-dependent red and blue detuned laser beams with beam waist w_0 . For optimum energy pumping, a *fixed* modulation frequency should be used, with a value close to the soliton frequency.

Dissipationless Regime: Consider first the case of no dissipation (Eq. (1)). The motion and stability of a quasi-1D dark soliton is well parametrized by its energy $E(\rho, z)$, calculated by integrating the energy functional, $\varepsilon(\psi) = \hbar^2/(2m) |\nabla\psi|^2 + V|\psi|^2 + (g/2)|\psi|^4$, across a conveniently defined soliton region and subtracting the corresponding contribution of the background fluid [13, 14, 27]. In order to facilitate a direct comparison of the soliton decay to the analytical homogeneous 1D soliton energy, the soliton dynamics are parametrized in terms of the ‘on-axis’ soliton energy $E_s = \int E(0, z) dz$ integrated over the region $(z_s \pm 5\xi)$, where z_s the instantaneous soliton position. In the absence of V_D , the soliton oscillates at $\omega_{\text{sol}} = \omega_z/\sqrt{2}$ [9, 10, 11, 12, 13, 14, 15, 16], emitting sound waves which oscillate at the trap frequency ω_z . This frequency mismatch means that the soliton propagates through a periodically modulated background density, with which it interacts continuously. Such interaction leads to a *weak* periodic modulation of the soliton energy, with the amplitude of such modulation further enhanced by the coupling between longitudinal and transverse degrees of freedom [11, 13] (Fig. 2(a), curves (i)).

To demonstrate substantial energy transfer into the soliton, we start with a low energy shallow soliton (speed $v = 0.75c$). Applying the drive potential induces an *additional* periodic background density modulation and a time-dependence in the soliton oscillation frequency, which is found to vary by no more than 10% around its unperturbed value ω_{sol} . The soliton initially gains energy and slows down, until the soliton and sound waves

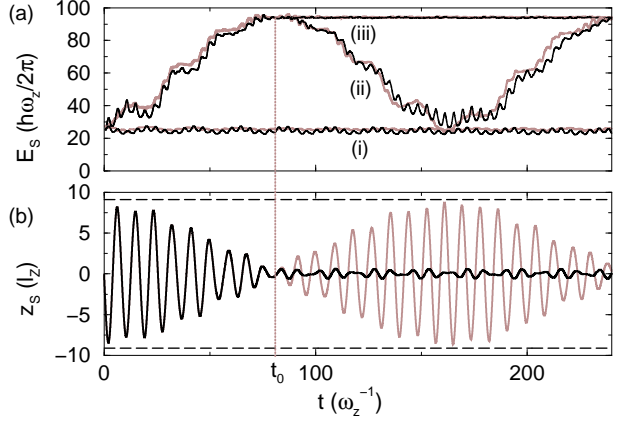


FIG. 2: ‘On axis’ quasi-1D soliton energy for (i) undriven case, (ii) continuous driving and (iii) driving switched off at $t_0 = 80\omega_z^{-1}$, based on simulations of the 3D cylindrically-symmetric GPE (black lines) and 1D GPE (grey lines) for a soliton with initial speed $v = 0.75c$. (b) Longitudinal soliton oscillations with continuous driving (grey line), and driving switched off at t_0 (vertical grey line) under the 3D GPE. Dashed lines indicate corresponding amplitude in absence of driving. The trap strength is determined from the chemical potential of the system: Quasi-1D: $\mu_{3D} = 8\hbar\bar{\omega}$ where $\bar{\omega} = (\omega_z\omega_{\perp}^2)^{1/3}$ and $\omega_{\perp}/\omega_z = 250$. Pure 1D: $\mu_{1D} = 70\hbar\omega_z$ for which the 1D density matches the quasi-1D longitudinal density. Drive parameters: $\omega_D = 0.98\omega_{\text{sol}}$, $\alpha = 0.1\mu_{1D}$, $w_0 = 3.2l_z$ and $z_0 = 10.7l_z$ where $l_z = \sqrt{\hbar/(m\omega_z)}$ the longitudinal harmonic oscillator length.

become out of phase and no longer interfere constructively. The soliton then starts losing energy (speeding up), until it comes back into phase, and the cycle repeats itself, as demonstrated by curves (ii) in Fig. 2(a). This figure illustrates the good agreement between the 3D ‘on-axis’ energy (black lines) and the corresponding energy of the pure 1D simulations (grey lines) (the 3D results feature an additional small amplitude oscillation due to longitudinal-transverse coupling). The corresponding beating in the soliton amplitude is shown in Fig. 2(b) (grey line). This beating effect can be essentially visualized as the periodic cycling between two possible states of the system, one being the initial fast (low energy) dark soliton, and the other being a stationary black (high energy) soliton. The above picture is analogous to the cycling of a driven condensate between the ‘no-vortex’ and ‘single-vortex’ configurations [29].

A soliton of greatly reduced speed (higher energy) can be created by removing the drive potential at the point of maximum energy transfer in the cycle. For suitably optimized drive parameters, we find that the residual oscillations (curves (iii) in Fig. 2(a)) of the soliton energy are smaller than the energy modulation in the absence of driving (curves (i) in same figure). The corresponding decrease of soliton oscillation amplitude is shown by the black line in Fig. 2(b).

The soliton dynamics depend rather sensitively on the parameters of the driving field which should be care-

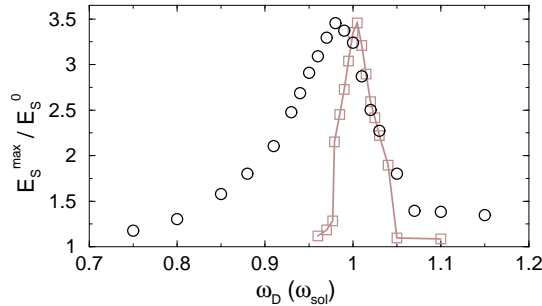


FIG. 3: Ratio of maximum pumped energy E_s^{\max} to initial soliton energy E_s^0 for a soliton with initial speed $v = 0.75c$ in the presence of optimized driving as a function of drive frequency (in units of the unperturbed soliton frequency $\omega_{\text{sol}} = \omega_z/\sqrt{2}$) for (i) no damping (black circles), or (ii) with damping $\gamma = 5 \times 10^{-4}$ (grey squares). This value of γ leads to the same soliton lifetime as for the undriven $0.3c$ soliton in Fig. 4. Results based on pure 1D GPE for the case of Fig. 2.

fully optimized for these effects to be clearly observable. Firstly, the pumping should take place outside of the range of the soliton oscillations (i.e. $z_0 > 9l_z$ for $v = 0.75c$). If this is not the case, the soliton traverses the gaussian bumps, leading to ‘dephasing’ of emitted sound waves and subsequent decay of the soliton [14]. The amount of energy transferred to the soliton depends on the drive potential seen by the soliton at the extrema of its oscillatory motion. This parameter depends directly on the drive frequency ω_D , the amplitude of the potential modulation α , the range of the potential w_0 , its location z_0 , and the initial soliton speed v . If all but one of the above parameters are kept constant, then there is a resonance around an optimum value of that parameter. This resonance is illustrated for the drive frequency ω_D by the open circles in Fig. 3. Note that the maximum pumping does not arise at ω_{sol} , due to the additional frequency modification induced by the perturbing potential; however, the optimum frequency is consistently found to lie close to (and smaller than) the unperturbed frequency. Importantly, the width of the resonance for which the transferred soliton energy reaches half its maximum value (FWHM), is reasonably broad, of the order of 10% the soliton frequency.

Dissipative Regime In a realistic quasi-1D system (where the snake-instability [8] is suppressed on timescales of interest), both the condensate and the soliton will be prone to damping, e.g. due to the presence of a small thermal cloud [16]. A first estimate into the effect of dissipation can be obtained by introducing a phenomenological damping term $\hbar\gamma\partial\psi/\partial t$ on the left hand side of Eq. (1). In the absence of driving, this term leads to an approximately exponential decay of the soliton energy, modified by the oscillatory motion of the soliton (dashed lines in Fig. 4(a)), and an accompanying increase in the soliton oscillation amplitude (Fig. 4(b), dashed lines) [9, 13]. The soliton lifetime is determined by the decay constant γ . By pumping energy into the

soliton, we can attempt to stabilize it against such dissipative losses.

To evaluate the effectiveness of stabilization, we choose to study a high energy, low speed soliton, and investigate whether parametric driving can extend its lifetime. The effect of the drive potential in the presence of damping is shown by the solid lines in Fig. 4(a): the soliton maintains a nearly constant energy in this timescale, whereas the same soliton would have completely decayed in the absence of driving (dashed lines in same figure). For sufficiently large decay constants, the dark soliton will eventually decay, even in the presence of the drive potential, but its lifetime can nonetheless be significantly extended (roughly doubled in the example of Fig. 4). The parameters which can be monitored experimentally are the amplitude and period of the soliton oscillations, and the soliton depth [6]. As shown clearly in Fig. 4(b), the oscillation amplitude in quasi-1D condensates (solid black line) remains essentially unaffected from the undamped undriven case (denoted by horizontal solid grey lines), and is clearly distinct from the undriven dissipative motion (dashed lines), whose amplitude increases. Hence, periodic monitoring of soliton oscillations (e.g. via repeated time of flight measurements) offers a direct experimental demonstration of parametric driving. Dissipation damps both the soliton and sound field, and the latter leads to a narrowing of the resonance in the drive frequency (grey data in Fig. 3).

We have also investigated alternative schemes for pumping energy into the system. For example, using one off-centre paddle, or inverting the sign in Eq. (3) (i.e. $\alpha < 0$), leads to a less efficient energy transfer, while periodically displacing the trap leads to no net increase in the soliton energy. Although additional tricks (e.g.

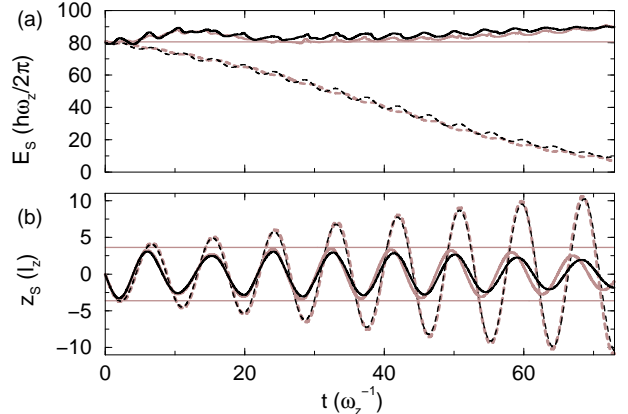


FIG. 4: (a) Energy of a slow soliton of initial speed $v = 0.3c$ for a dissipative system ($\gamma = 10^{-3}$) in the presence (solid lines) or absence (dashed lines) of a pump ($\omega_D = \omega_{\text{sol}}$, $z_0 = 7.1l_z$) showing both quasi-1D (black) and pure 1D (grey) results. (b) Corresponding trajectories. Horizontal solid lines indicate the corresponding undamped undriven results for (a) energy and (b) amplitude of soliton oscillations. Other parameters as in Fig. 2.

moving the paddles out as the soliton approaches them, turning the pump on and off at certain times) could be employed to further enhance the lifetime extension, their effectiveness was found to depend sensitively on the particular parameters used. Moreover, approximately locking the drive frequency to the time-varying soliton frequency via numerical feedback is not an efficient means of energy pumping, highlighting the importance of a slight frequency mismatch between the soliton and the drive potential.

Finally, we discuss the relevance of the proposed scheme to current experiments with atomic BECs. Given a longitudinal confinement $\omega_z = 2\pi \times 10$ Hz, the presented results correspond to $\omega_{\perp} = 2\pi \times 2500$ Hz and a linear ‘on-axis’ density $n = 5 \times 10^7 (1.5 \times 10^7)$ m⁻¹ of ²³Na (⁸⁷Rb). The harmonic oscillator time unit is $\tau \approx 15$ ms. In the dissipative example of Fig. 4 with $\gamma = 10^{-3}$, this would correspond to a soliton lifetime of around 1 s, which is consistent with the theoretical predictions for solitons in highly elongated three-dimensional geometries [9, 10, 16]. The paddle beams have a waist $w_0 = 20$ μ m and maximum amplitude $\alpha = 7\hbar\omega_z$ lo-

cated around $z_0 = 7l_z$. We have also verified that the results presented here hold for smaller aspect ratios (e.g. $\omega_{\perp}/\omega_z = 50$). Since, for a given aspect ratio, higher frequencies correspond to faster timescales, the technique presented here is not sensitive to the particular soliton lifetime. There is, however, an upper limit of γ (corresponding to large dissipation), beyond which it becomes practically impossible to pump energy into the system.

In summary, we have shown that, in the case of a dark soliton oscillating in a harmonically trapped Bose-Einstein condensate, the addition of two out of phase gaussian potentials, with amplitude modulated periodically at a fixed frequency close to the soliton frequency, leads to pumping of energy into the soliton. This technique, which bears close analogies to the parametric driving used in other systems, can stabilize the soliton against decay for timescales up to a few times its natural lifetime. This effect should be experimentally observable in current experiments, given suitable optimization of the driving potential.

We acknowledge discussions with D.J. Frantzeskakis and P.G Kevrekidis and the U.K. EPSRC for funding.

[1] Y. S. Kivshar and B. Luther-Davies, Phys. Rep. **278**, 81-197 (1998).
[2] D. Krökel, N. J. Halas, G. Giuliani, and D. Grischkowsky, Phys. Rev. Lett. **60**, 29 (1998).
[3] G. A. Swartzlander Jr. *et al.*, Phys. Rev. Lett. **66**, 1583 (1991).
[4] B. Denardo, W. Wright, S. Putterman, and A. Larraza, Phys. Rev. Lett. **64**, 1518 (1990).
[5] M. Chen, M. A. Tsankov, J. M. Nash, and C. E. Patton, Phys. Rev. Lett. **70**, 1707 (1993).
[6] S. Burger *et al.*, Phys. Rev. Lett. **83**, 5198 (1999); J. Denschlag *et al.*, Science **287**, 97 (2000); Z. Dutton, M. Budde, C. Slowe, and L. V. Hau, Science **293**, 663 (2001).
[7] A. V. Mamaev, M. Saffman, and A. A. Zozulya, Phys. Rev. Lett. **76**, 2262 (1996).
[8] D. L. Feder *et al.*, Phys. Rev. A **62**, 053606 (2000); B.P. Anderson *et al.*, Phys. Rev. Lett. **86**, 2926 (2001); J. Brand and W. Reinhardt, Phys. Rev. A **65**, 043612 (2002).
[9] T. Busch and J. R. Anglin, Phys. Rev. Lett. **84**, 2298 (1999).
[10] A. E. Muryshev, H. B. van Linden van den Heuvell, and G. V. Shlyapnikov, Phys. Rev A **60**, R2665 (1999).
[11] G. Huang, J. Szeftel, and S. Zhu, Phys. Rev. A **65**, 053605 (2002).
[12] D. J. Frantzeskakis *et al.*, Phys. Rev. A **66**, 053608 (2002).
[13] N. G. Parker, N. P. Proukakis, M. Leadbeater, and C. S. Adams, Phys. Rev. Lett. **90**, 220401 (2003).
[14] N. G. Parker, N. P. Proukakis, M. Leadbeater, and C. S. Adams, J. Phys. B **36**, 2891 (2003); N. G. Parker *et al.* J. Phys. B (In Press, 2004), cond-mat/0310759 (2003); N.P. Proukakis *et al.*, J. Opt. B (In Press), cond-mat/0311141 (2003).
[15] V. A. Brazhnyi and V. V. Konotop, Phys. Rev. A **68**, 043613 (2003).
[16] P.O. Fedichev, A.E. Muryshev and G.V. Shlyapnikov, Phys. Rev. A **60**, 3220 (1999); A. E. Muryshev *et al.*, Phys. Rev. Lett. **89**, 110401 (2002).
[17] J. Dziarmaga, Z. P. Karkuszewski, and K. Sacha, J. Phys. B **36**, 1217 (2003).
[18] Y. S. Kivshar and B. A. Malomed, Rev. Mod. Phys. **61**, 763 (1989).
[19] C. Elphick and E. Meron, Phys. Rev. A **40**, 3226 (1989).
[20] F. K. Abdullaev and S. K. Tadjimuratov, Opt. Comm. **116**, 179 (1995).
[21] A. D. Kim, W. L. Kath and C. G. Goedde, Opt. Lett. **21**, 465 (1996).
[22] P. Coullet, J. Lega, B. Houchmanzadeh, and J. Lajzerowicz, Phys. Rev. Lett. **65**, 1352 (1990); D.V. Skryabin *et al.*, Phys. Rev. E **64**, 056618 (2001).
[23] I.V. Barashenkov, S.R. Woodford and E.V. Zemlyanaya, Phys. Rev. Lett. **90**, 054103 (2003).
[24] A. Goerlitz *et al.*, Phys. Rev. Lett **87**, 130402 (2001); F. Schreck *et al.* Phys. Rev. Lett. **87**, 080403 (2001); H. Ott *et al.* Phys. Rev. Lett. **87**, 230401 (2001).
[25] F. Dalfovo, S. Giorgini, L. P. Pitaevskii, and S. Stringari, Rev. Mod. Phys. **71**, 463 (1999).
[26] V. E. Zakharov and A. B. Shabat, Zh. Eksp. Teor. Fiz. **64**, 1627 (1973).
[27] L. D. Carr, J. Brand, S. Burger, and A. Sanpera, Phys. Rev. A **63**, 051601 (2001).
[28] S. Choi, S. A. Morgan and K. Burnett, Phys. Rev. A **57**, 4057 (1998); M. Tsubota, K. Kasamatsu and M. Ueda, Phys. Rev. A **65**, 023603 (2002).
[29] B. M. Caradoc-Davies, R. J. Ballagh and K. Burnett, Phys. Rev. Lett. **83**, 895 (1999).